Design and Screening of Bimetallic Catalysts for Nitric Oxide Reduction by CO: A Study of Kinetic Monte Carlo Simulation Based on First-Principles Calculations

Caimu Wang,[1] Renyi Li,[1] and Wei Guo*,[1,2]

[1] *Centre for Quantum Physics, Key Laboratory of Advanced Optoelectronic Quantum Architecture and Measurement (MOE), School of Physics, Beijing Institute of Technology, Beijing 100081, China*

[2] *Frontiers Science Center for High Energy Material (MOE), Beijing Institute of Technology, Beijing 100081, China*

Supplementary Information

Table S1. The adsorption energies of the adsorptive species containing oxygen using different cutoff energies.

X*	Sites	Adsorption energies with different cutoff energy		
		350 eV	400 eV	450 eV
O*	f1	–2.57	–2.54	–2.53
O*	h2	–2.49	–2.46	–2.44
CO*	s1	–1.57	–1.54	–1.52
CO*	h2	–1.74	–1.71	–1.69
NO*	s2	–0.97	–0.95	–0.94
NO*	h1	–1.91	–1.89	–1.87

Table S2. The DFT energy differences were calculated for several structures, including the $Ni_{striped}$/Pt(111) surface and adsorptive species on this surface, using convergence criteria of 0.1 eV $Å^{-1}$ and 0.05 eV $Å^{-1}$ for force during ionic relaxations.

Structures	Difference (meV)
$Ni_{striped}$/Pt(111)	6.58
N* (f1 site)	6.65
O* (f1 site)	13.2
CO* (h2 site)	1.41
NO* (s2 site)	15.8

Table S3. The adsorption energies of the adsorptive species at different sites without/with D3 correction.

X*	sites	Without D3	With D3
O*	f1	–2.57	–2.55
O*	h2	–2.49	–2.51
CO*	s1	–1.57	–1.58
CO*	h2	–1.74	–1.76
NO*	s2	–0.97	–0.98
NO*	h1	–1.91	–1.93

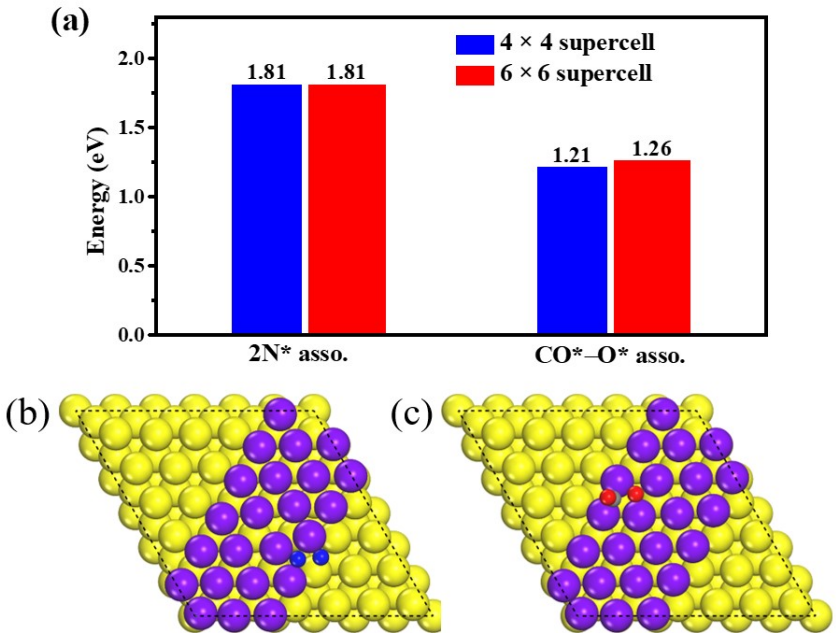

Figure S1. (a) Comparison of reaction barriers for the 2N* association and CO*-O* association on the 6 × 6 and 4 × 4 striped Ni-Pt-Pt (111) supercell surface. The transition states of (b) 2N* association and (c) CO*-O* association reaction on the 6 × 6 striped Ni-Pt-Pt (111) supercell surface.

Table S4. Vibrational frequencies for gas-phase and surface species. The "#" indicates transition state in the table.

Species	**Frequencies (cm^{-1})**
NO(g)	1896
N_2(g)	2405
O_2(g)	1542
CO(g)	2107

CO_2(g)	2334	1330	626	621					
NO*	871	465	457	323	255	235			
N*	483	481	468						
O*	441	420	306						
O_2*	558	435	308	285	247	209			
CO*	1683	310	265	253	143	119			
NO*$^{\#}$	504	473	403	390	259	499 *i*			
N_2*$^{\#}$	500	472	400	361	338	181 *i*			
O_2*$^{\#}$	555	383	292	269	44	198 *i*			
$CO_2^{\#}$	1709	572	371	318	288	216	88	68	456 i

Table S5. The reversible elementary steps for various reaction sites in the KMC simulation.

Index	Reaction	Sites	Barriers	Pre-exponential	Pre-ratio
1	N* diff.	h2, f2	1.8	6.21E+12	1.0
2	N* diff.	f2, h1	1.7	6.21E+12	1.0
3	N* diff.	f1, h1	1.8	6.21E+12	1.0
4	N* diff.	f3, s2	1.0	6.21E+12	1.0
5	N* diff.	s2, h2	0.6	6.21E+12	1.0
6	N* diff.	f3, s1	1.0	6.21E+12	1.0
7	N* diff.	s1, f1	0.65	6.21E+12	1.0
8	N* diff.	f3, s3	1.0	6.21E+12	1.0
9	N* diff.	s3, s1	1.0	6.21E+12	1.0
10	O* diff.	h2, f2	1.8	6.21E+12	1.0
11	O* diff.	f2, h1	1.8	6.21E+12	1.0
12	O* diff.	f1, h1	1.8	6.21E+12	1.0
13	O* diff.	f3, s2	1.0	6.21E+12	1.0
14	O* diff.	s2, h2	0.4	6.21E+12	1.0
15	O* diff.	f3, s2	1.0	6.21E+12	1.0
16	O* diff.	s1, f1	0.5	6.21E+12	1.0
17	O* diff.	h3, f3	1.0	6.21E+12	1.0
18	O* diff.	h3, s1	1.0	6.21E+12	1.0
19	NO adso.	s1	0.0	2.82E+07	7.45E-10
20	NO adso.	s2	0.0	2.82E+07	7.45E-10
21	NO adso.	h1	0.0	2.82E+07	7.45E-10
22	NO adso.	h2	0.0	2.82E+07	7.45E-10
23	NO adso.	f1	0.0	2.82E+07	7.45E-10
24	NO adso.	f2	0.0	2.82E+07	7.45E-10

25	CO adso.	s1	0.0	2.92E+07	7.24E-09
26	CO adso.	s2	0.0	2.92E+07	7.24E-09
27	CO adso.	h1	0.0	2.92E+07	7.24E-09
28	CO adso.	h2	0.0	2.92E+07	7.24E-09
29	CO adso.	f1	0.0	2.92E+07	7.24E-09
30	CO adso.	f2	0.0	2.92E+07	7.24E-09
31	CO adso.	f3	0.0	2.92E+07	7.24E-09
32	CO adso.	h3	0.0	2.92E+07	7.24E-09
33	O_2 adso.	f1	0.0	2.74E+07	2.66E-09
34	O_2 adso.	f2	0.0	2.74E+07	2.66E-09
35	O_2 adso.	h1	0.0	2.74E+07	2.66E-09
36	O_2 adso.	h2	0.0	2.74E+07	2.66E-09
37	NO diss.	f3, s2, h2	0.41	1.74E+13	0.70
38	NO diss.	f3, s1, f1	0.42	1.74E+13	0.70
39	NO diss.	h3, s1, f1	0.43	1.74E+13	0.70
40	NO diss.	f1, h1, f2	0.74	1.74E+13	0.70
41	NO diss.	f2, h1, f1	0.70	1.74E+13	0.70
42	NO diss.	h1, f2, h2	0.77	1.74E+13	0.70
43	NO diss.	h2, f2, h1	0.79	1.74E+13	0.70
44	NO diss.	h1, f1, h1	0.87	1.74E+13	0.70
45	NO diss.	f1, h1, f1	0.66	1.74E+13	0.70
46	NO diss.	f2, h2, f2	0.77	1.74E+13	0.70
47	NO diss.	h2, f2, h2	0.69	1.74E+13	0.70
48	NO diss.	s1, f1, h1	1.11	1.74E+13	0.70
49	NO diss.	s2, h2, f2	1.32	1.74E+13	0.70
50	O_2 diss.	f1, h1, f2	0.26	5.21E+13	0.30
51	O_2 diss.	h1, f2, h2	0.06	5.21E+13	0.30
52	O_2 diss.	h1, f1, h1	0.02	5.21E+13	0.30
53	O_2 diss.	f1, h1, f1	0.31	5.21E+13	0.30
54	O_2 diss.	f2, h2, f2	0.15	5.21E+13	0.30
55	O_2 diss.	h2, f2, h2	0.17	5.21E+13	0.30
56	N_2 asso.	f1, h1, f2	2.24	4.82E+13	1.65E+06
57	N_2 asso.	h1, f2, h2	2.21	4.82E+13	1.65E+06
58	N_2 asso.	h1, f1, h1	2.08	4.82E+13	1.65E+06
59	N_2 asso.	f1, h1, f1	2.30	4.82E+13	1.65E+06
60	N_2 asso.	f2, h2, f2	2.17	4.82E+13	1.65E+06
61	N_2 asso.	h2, f2, h2	2.35	4.82E+13	1.65E+06
62	N_2 asso.	s1, f1, h1	1.65	4.82E+13	1.65E+06
63	N_2 asso.	s2, h2, f2	1.31	4.82E+13	1.65E+06
64	N_2 asso.	f3, s2, h2	1.37	4.82E+13	1.65E+06
65	N_2 asso.	f3, s1, f1	1.14	4.82E+13	1.65E+06
66	N_2 asso.	h3, s1, f1	1.13	4.82E+13	1.65E+06
67	N_2 asso.	h3, f3, s2	0.30	4.82E+13	1.65E+06
68	CO_2 asso.	h1, f2, h2	2.10	2.31E+13	9.88E+05

69	CO_2 asso.	h2, f2, h1	1.93	2.31E+13	9.88E+05
70	CO_2 asso.	h2, f2, h2	2.20	2.31E+13	9.88E+05
71	CO_2 asso.	f2, h2, f2	1.97	2.31E+13	9.88E+05
72	CO_2 asso.	f2, h1, f1	2.16	2.31E+13	9.88E+05
73	CO_2 asso.	f1, h1, f2	2.05	2.31E+13	9.88E+05
74	CO_2 asso.	f1, h1, f1	2.25	2.31E+13	9.88E+05
75	CO_2 asso.	h1, f1, h1	1.84	2.31E+13	9.88E+05
76	CO_2 asso.	s1, f1, h1	1.60	2.31E+13	9.88E+05
77	CO_2 asso.	s2, h2, f2	1.99	2.31E+13	9.88E+05
78	CO_2 asso.	h1, f1, s1	1.06	2.31E+13	9.88E+05
79	CO_2 asso.	f2, h2, s2	1.32	2.31E+13	9.88E+05
80	CO_2 asso.	f3, s1, f1	1.56	2.31E+13	9.88E+05
81	CO_2 asso.	f1, s1, f3	0.33	2.31E+13	9.88E+05
82	CO_2 asso.	f1, s1, h3	0.72	2.31E+13	9.88E+05
83	CO_2 asso.	f3, s2, h2	1.45	2.31E+13	9.88E+05
84	CO_2 asso.	h2, s2, f3	0.27	2.31E+13	9.88E+05
85	CO_2 asso.	s2, f3, h3	0.78	2.31E+13	9.88E+05
86	CO_2 asso.	h3, s1, f1	1.76	2.31E+13	9.88E+05
87	CO_2 asso.	h3, f3, s2	0.92	2.31E+13	9.88E+05

Table S6. The pair interactions between the first and second nearest neighbors of two entities, involving all surface species (N*, O*, NO*, CO*, O_2*).

Pair	Sites	Energy (eV)	Pair	Sites	Energy (eV)
N*–O* (1st)	h1, f1	3.01	NO*–N* (2ed)	s1, s2	0.24
N*–O* (1st)	f1, h1	2.95	NO*–N* (2ed)	s2, f2	0.26
N*–O* (1st)	f2, h2	2.71	NO*–N* (2ed)	f1, f2	0.29
N*–O* (1st)	h1, f2	2.26	NO*–N* (2ed)	f1, h3	0.31
N*–O* (1st)	h2, f2	2.91	NO*–O* (1st)	s2, h2	4.59
N*–O* (1st)	s1, f1	2.19	NO*–O* (1st)	s1, f1	4.68
N*–O* (1st)	h2, s2	1.23	NO*–O* (1st)	s2, f3	3.98
N*–O* (1st)	f1, s1	1.46	NO*–O* (1st)	s1, f3	4.15
N*–O* (1st)	h3, s1	1.67	NO*–O* (1st)	s1, h3	4.22
N*–O* (1st)	s2, f3	1.32	NO*–O* (2ed)	s1, h1	0.31
N*–O* (1st)	h2, s2	1.23	NO*–O* (2ed)	s1, s2	0.35
N*–O* (1st)	f3, s1	1.67	NO*–O* (2ed)	s2, f2	0.28
N*–O* (1st)	h3, f3	1.67	NO*–O* (2ed)	f1, f2	0.37

N*–O* (2ed)	f3, h2	0.02	NO*–O* (2ed)	f1, h3	0.44
N*–O* (2ed)	f1, f3	0.03	NO*–NO* (1st)	s2, h2	4.6
N*–O* (2ed)	h1, h1	0.28	NO*–NO* (1st)	s1,f1	4.5
N*–O* (2ed)	h2, h2	0.27	NO*–NO* (1st)	f1, h1	4.1
N*–O* (2ed)	f1, f1	0.25	NO*–NO* (1st)	h1, f2	3.9
N*–O* (2ed)	f2, f2	0.22	NO*–NO* (1st)	f2, h2	4.3
N*–O* (2ed)	f1, f2	0.20	NO*–NO* (2ed)	s1, s2	0.62
N*–O* (2ed)	h2, h1	0.25	NO*–NO* (2ed)	s2, f2	0.61
N*–N* (1st)	s2, h2	1.13	NO*–NO* (2ed)	s1, h1	0.59
N*–N* (1st)	f1, s1	1.57	NO*–NO* (2ed)	h1, h2	0.64
N*–N* (1st)	s1, h3	2.20	NO*–NO* (2ed)	f1, f2	0.54
N*–N* (1st)	f2, h1	2.18	NO*–NO* (2ed)	f1, f1	0.41
N*–N* (1st)	h1, f1	2.07	CO*–CO* (1st)	f2, h1	3.00
N*–N* (1st)	h2, f2	2.08	CO*–CO* (1st)	f2, h2	2.71
N*–N* (1st)	s2, f3	2.71	CO*–CO* (1st)	h1, f1	4.50
N*–N* (2ed)	f1, f2	0.28	CO*–CO* (1st)	s2, h2	2.70
N*–N* (2ed)	h1, h2	0.32	CO*–CO* (1st)	s1, f1	3.30
N*–N* (2ed)	h1, h1	0.43	CO*–CO* (2ed)	f1, f1	0.20
N*–N* (2ed)	f1, f1	0.30	CO*–CO* (2ed)	f2, f2	0.18
N*–N* (2ed)	f2, f2	0.32	CO*–CO* (2ed)	h1, h1	0.22
N*–N* (2ed)	h2, h2	0.35	CO*–CO* (2ed)	h2, h2	0.20
N*–N* (2ed)	s1, h1	-0.06	CO*–CO* (2ed)	f1, f2	0.19
N*–N* (2ed)	s2, f2	0.07	NO*–CO* (1st)	s1, f1	3.13
N*–N* (2ed)	f3, h2	0.05	NO*–CO* (1st)	f1, s1	3.01
N*–N* (2ed)	h3, f1	0.004	NO*–CO* (1st)	s2, h2	3.35
O*–O* (1st)	f2, h1	3.63	NO*–CO* (2ed)	s2, f2	0.17
O*–O* (1st)	h1, f1	2.81	NO*–CO* (2ed)	f2, s2	0.18
O*–O* (1st)	h2, f2	2.94	NO*–CO* (2ed)	s1, h1	0.15
O*–O* (1st)	f1, s1	1.10	CO*–N* (1st)	f1, h1	2.33
O*–O* (1st)	s2, h2	3.14	CO*–N* (1st)	f1, s1	2.53
O*–O* (1st)	s1, h3	3.20	CO*–N* (2ed)	s1, h1	0.13
O*–O* (2ed)	f1, f1	0.22	O_2*–O_2* (1st)	f1, h1	4.88
O*–O* (2ed)	h1, h1	0.21	O_2*–O_2* (2ed)	f1, f2	0.88
O*–O* (2ed)	f2, f2	0.16	O_2*–N* (1st)	f1, h1	4.49
O*–O* (2ed)	h2, h2	0.27	O_2*–N* (1st)	h1, f1	3.20

O*–O* (2ed)	f1, f2	0.24	O_2*–N* (2ed)	f1, f2	0.90
O*–O* (2ed)	h1, h2	0.02	O_2*–O* (1st)	f1, h1	4.3
O*–O* (2ed)	s2, f2	0.15	O_2*–O* (1st)	h1, f1	3
O*–O* (2ed)	h3, f1	0.11	O_2*–O* (2ed)	f1, f2	0.91
O*–O* (2ed)	f3, h2	0.01	O_2*–NO* (1st)	f1, h1	4.29
O*–O* (2ed)	f3, f1	0.03	O_2*–NO* (1st)	f2, h1	3.65
NO*–N* (1st)	s2, h2	3.57	O_2*–NO* (2ed)	f1, f2	1.51
NO*–N* (1st)	s1, f1	3.86	O_2*–CO* (1st)	f1, h1	4.61
NO*–N* (1st)	s2, f3	2.98	O_2*–CO* (1st)	f2, h1	3.32
NO*–N* (1st)	s1, f3	3.44	O_2*–CO* (2ed)	f1, f1	1.12
NO*–N* (1st)	s1, h3	2.96	O_2*–CO* (2ed)	h1, h2	1.09
NO*–N* (2ed)	s1, h1	0.28	O_2*–CO* (2ed)	f1, f2	1.26

Table S7. The adsorption energies of N_2 and CO_2 at step/edge sites on several striped bimetallic surfaces.

Species	**Sites**	**Ads. energy**	**Species**	**Sites**	**Ads. energy**
N_2	f1 (Ni/Pt)	0.06	CO_2	f1 (Ni/Pt)	0.31
N_2	h2 (Ni/Pt)	–0.15	CO_2	h2 (Ni/Pt)	–0.07
N_2	s1 (Ni/Pt)	0.41	CO_2	s1 (Co/Pt)	0.22
N_2	f1 (Co/Pt)	–0.02	CO_2	f1 (Co/Pt)	–0.26
N_2	h2 (Co/Pt)	–0.11	CO_2	s1 (Fe/Pd)	–0.30
N_2	f1 (Fe/Pd)	–0.19	CO_2	f1 (Fe/Pd)	–0.24
N_2	h2 (Fe/Pd)	–0.09	CO_2	h2 (Fe/Pd)	–0.10
N_2	s1 (Ni/Pd)	0.40	CO_2	s1 (Ni/Pd)	0.43
N_2	s2 (Ni/Pd)	0.33	CO_2	s2 (Ni/Pd)	0.15
N_2	f1 (Ni/Pd)	–0.10	CO_2	f1 (Ni/Pd)	–0.14
N_2	h2 (Ni/Pd)	–0.08	CO_2	h2 (Ni/Pd)	–0.10
N_2	f1(Ni/Ir)	0.04	CO_2	s1 (Ni/Ir)	–0.33
N_2	h2 (Ni/Ir)	0.16	CO_2	f1 (Ni/Ir)	0.02
N_2	f1 (Fe/Ag)	–0.04	CO_2	h2 (Ni/Ir)	–0.04
N_2	h2 (Fe/Ag)	0.05	CO_2	s1 (Fe/Ag)	–1.39
			CO_2	f1 (Fe/Ag)	–0.81
			CO_2	h2 (Fe/Ag)	–0.85

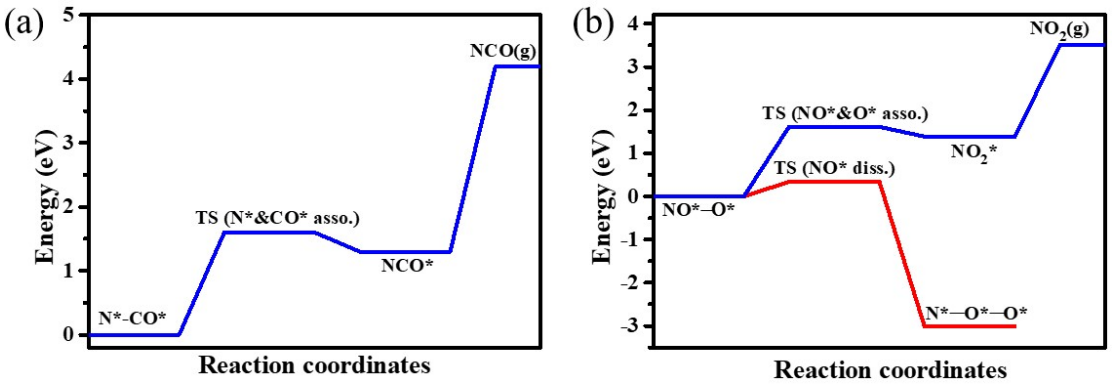

Figure S2 (a) Energy profile of CO* and N* association on the striped Ni-Pt-Pt (111) surface. (b) The comparison for energy profile of NO* and O* association and NO* dissociation on the striped Ni-Pt-Pt (111) surface.

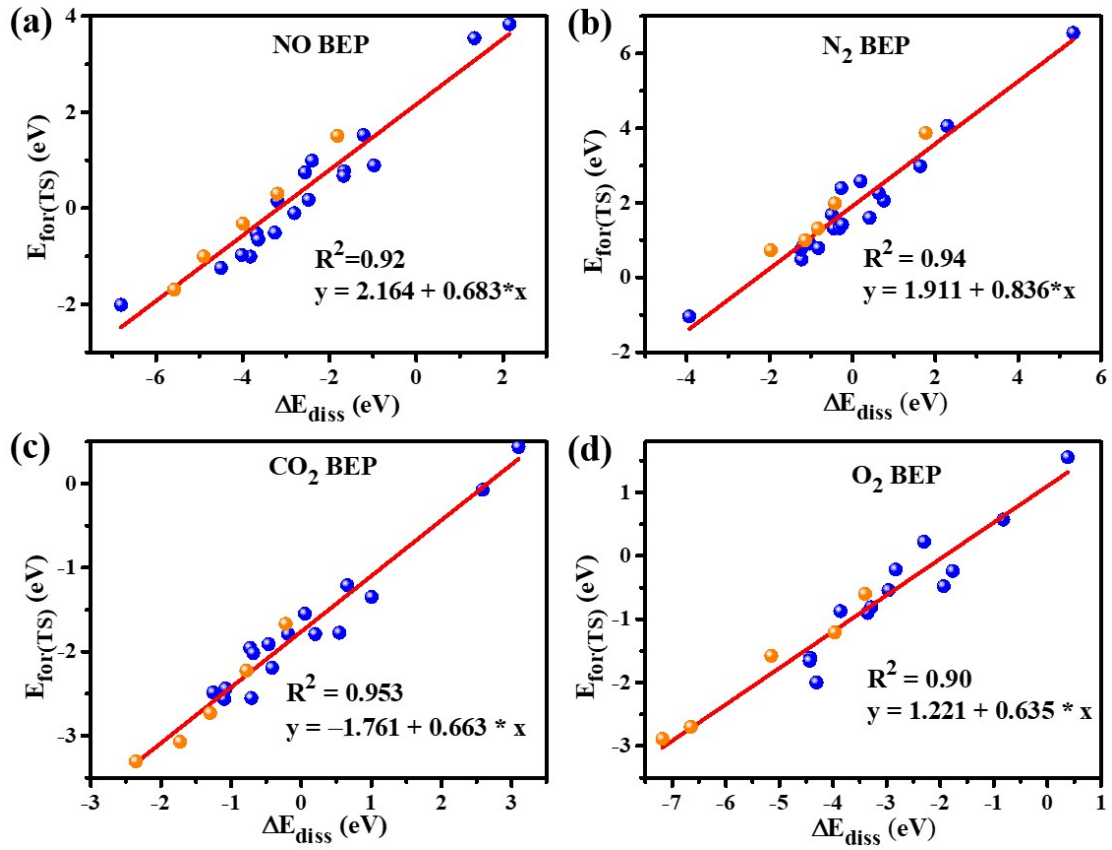

Figure S3. The BEP relationship between the reaction energies and the formation energies of transition states during the dissociative chemisorption of NO(g), N_2(g), CO_2(g), and O_2(g). The blue balls are the previously calculated data on (211) surfaces of pure metals[1]. The orange balls are our own calculations on multiple striped bimetallic surfaces.

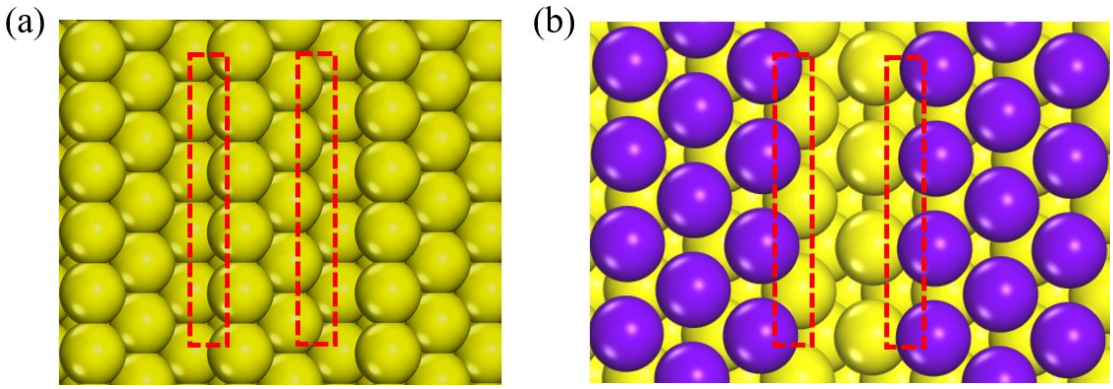

Figure S4. Structures of (a) transition metal (211) surface and (b) designed striped X-Y-Y bimetallic surface.

Table S8. The predicted formation energy of transition states with BEP relation and the DFT calculated data.

Surface	NO diss.		N2 diss.		CO_2 diss.		O_2 diss.	
	BEP	DFT	BEP	DFT	BEP	DFT	BEP	DFT
Ni-Pt-Pt	–0.50	–0.38	1.27	1.31	–2.65	–2.70	–1.81	–1.57
Cu-Pd-Pd	0.99	1.38	3.48	3.75	–1.88	–1.74	–0.81	–0.60
Rh-Ir-Ir	0.03	0.20	1.61	1.78	–2.25	–2.22	–1.17	–1.20
Fe-Pd-Pd	–1.12	–1.00	1.01	1.00	–2.91	–3.01	–2.72	–2.69
Fe-Ag-Ag	–1.67	–1.69	0.36	0.59	–3.31	–3.30	–2.98	–2.88

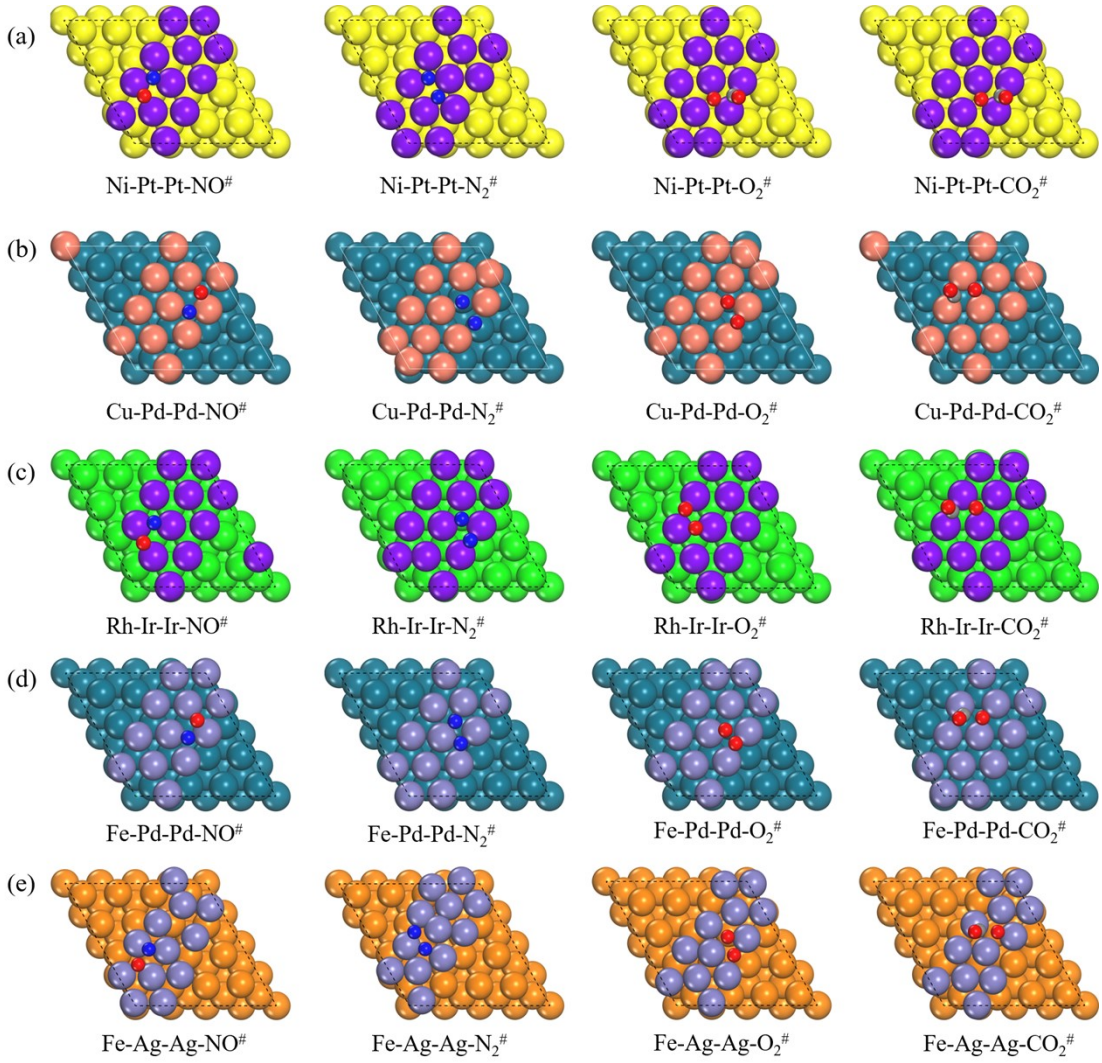

Figure S5. Structures of the transition states for NO dissociation, 2N* association, 2O* association, and the association of CO* and O*.

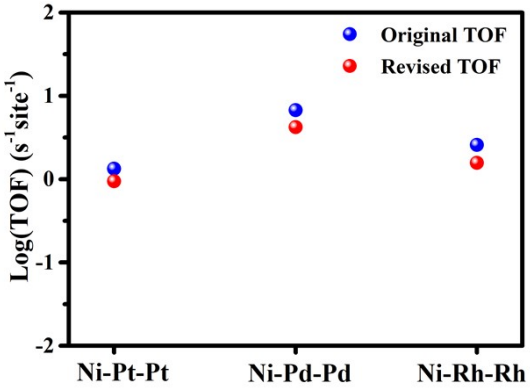

Figure S6. Comparison of original and revised TOF taking into account the error of BEP relationship for NO reduction reaction by CO. In the KMC simulations considering the BEP error, the barriers of NO* dissociation, 2N* association, and O_2* dissociation reaction were increased by 0.2 eV, and the association barrier of CO* and O* was increased by 0.05 eV compared with the original KMC

simulations.

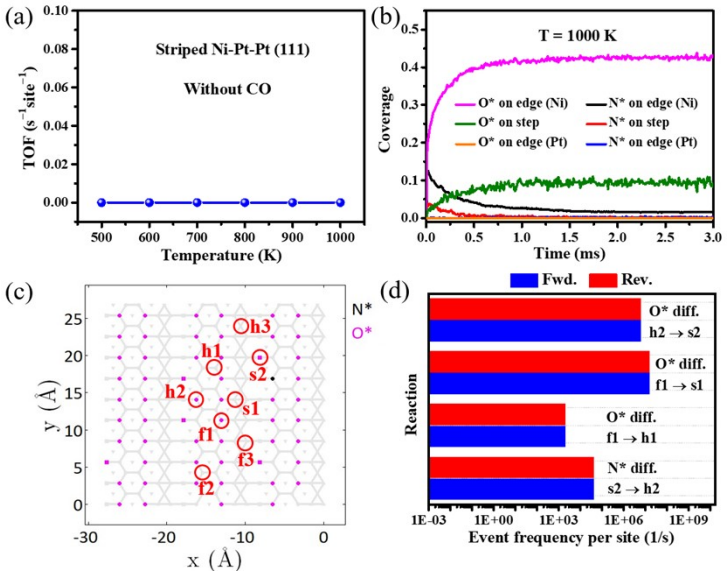

Figure S7. (a) The steady-state TOF of N_2 desorption about NO reduction reaction without CO on striped Ni-Pt-Pt (111) surface under different temperatures. (b) Coverage of N* and O* for the NO reduction reaction without CO at 1000 K on the striped Ni-Pt-Pt (111) surface. The Ni edge sites consist of the f1, f2, h1, and h2 sites, while the Pt edge sites consist of the f3 and h3 sites. The step sites are comprised of the s1 and s2 sites. (c) Representative snapshot of KMC simulation at the steady state on the striped Ni-Pt-Pt (111) surface. (d) Events in KMC simulation at the steady state.

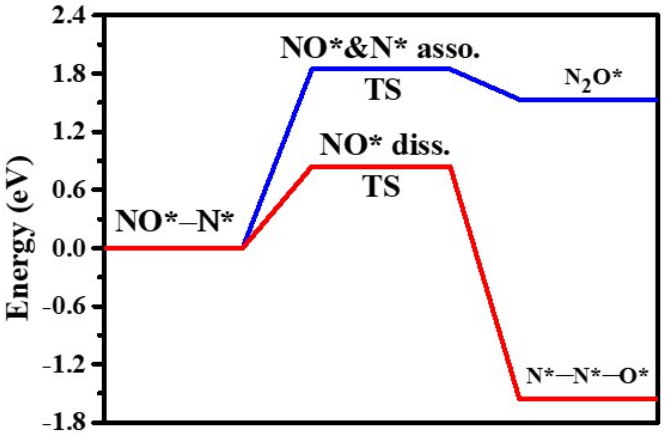

Figure S8. The energy profile of NO* and N* association and NO* dissociation when the co-adsorbed intermediate "N*-NO*" is present on the terraced Ni-Pt-Pt (111) surface.

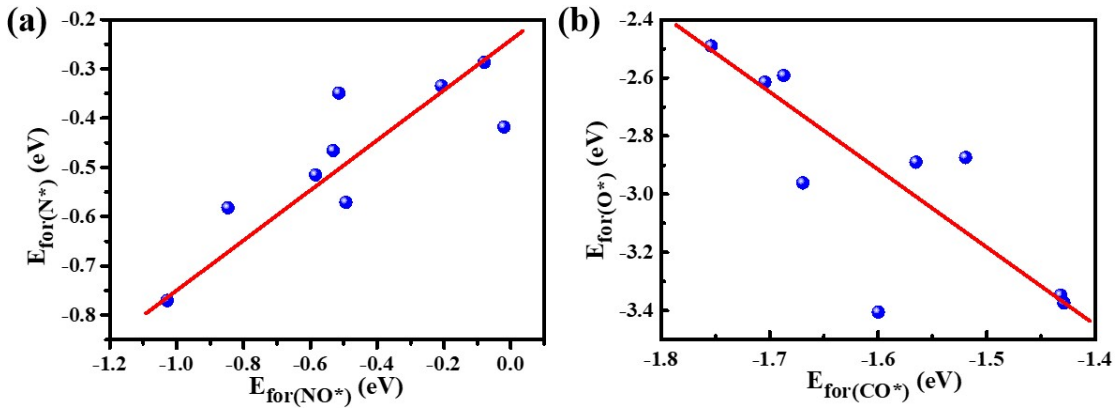

Figure S9. (a)The relation between the formation energies of NO* at step sites and 2N* at edge sites. (b) The relation between the formation energies of CO* at step and O* at edge sites.

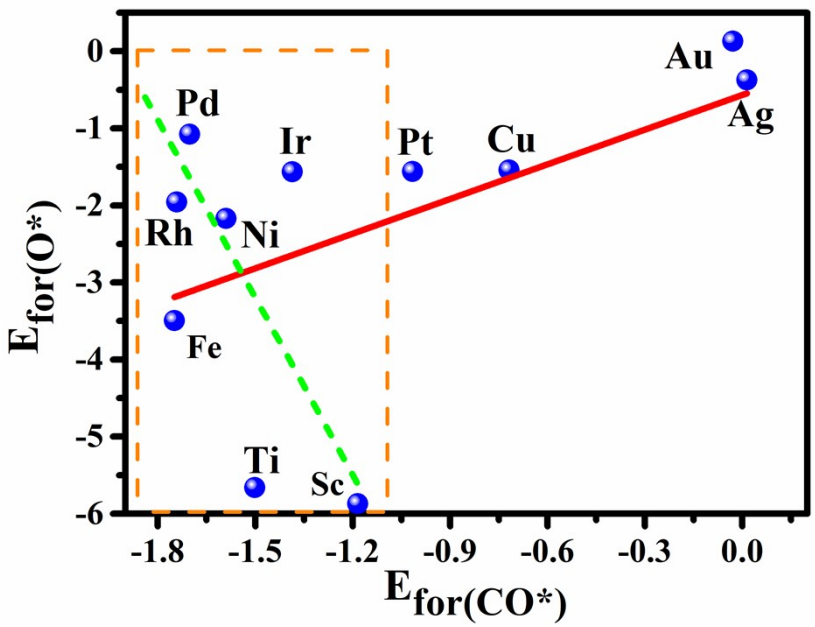

Figure S10. The relationship between the formation energies of CO* and O* located at the fcc-hollow site on a serial of transition metal (111) surfaces. The red line is the fitting line for all points. The green dotted line is the fitting line for the points in the orange square.

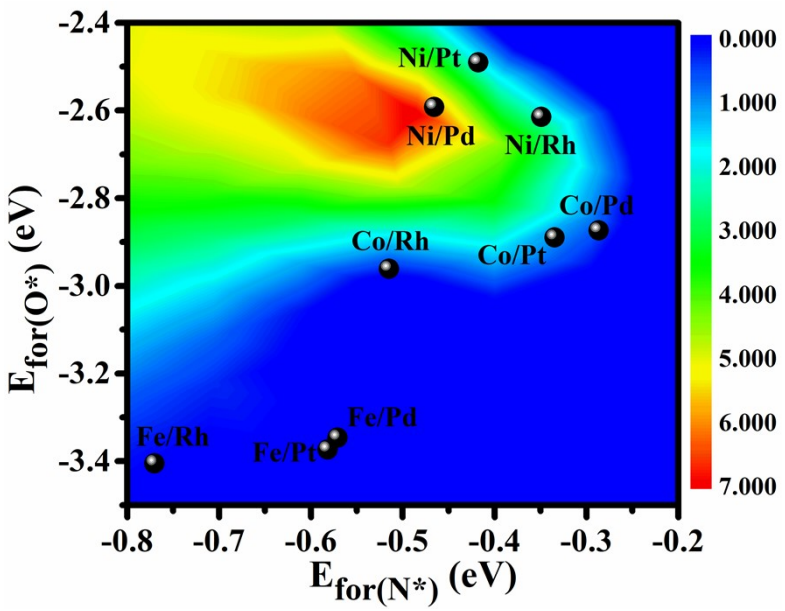

Figure S11. 2D volcano plot for NO reduction reaction by CO with the descriptors for the formation energies of N* and O* at the edge sites on the striped bimetallic surface.

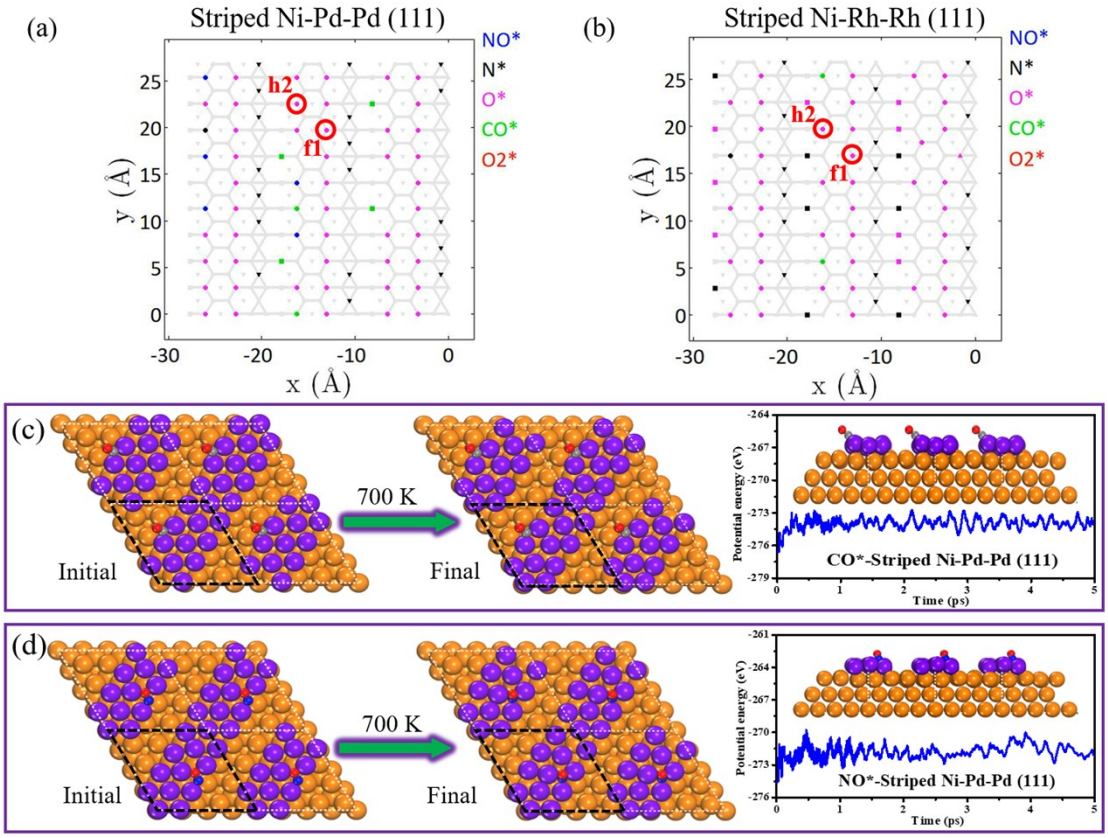

Figure S12. Representative snapshot of KMC simulation on (a) the striped Ni-Pd-Pd (111) surface and (b) the striped Ni-Rh-Rh (111) surface. AIMD simulations of striped Ni-Pd-Pd (111) surface with one adsorptive (c) CO and (d) NO molecule. The rightmost insets in show the potential energy fluctuation as a function of the simulated time. The side views of the final states are shown as insets

for illustrations. The orange, purple, green, gray, blue, and red spheres denote Pd, Ni, Rh, C, N, and O atoms, respectively.

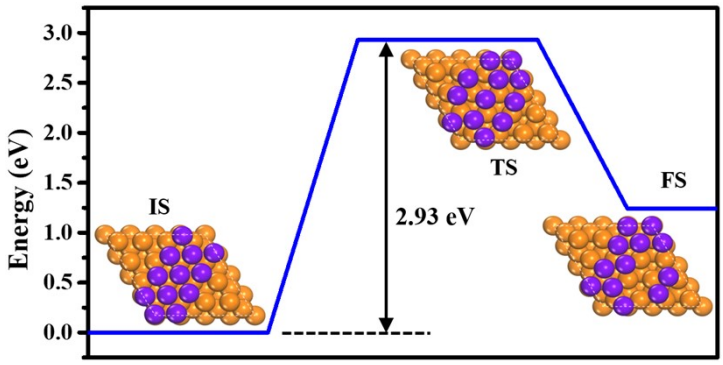

Figure S13. The minimum energy path for the diffusion of two Ni atoms on the striped Ni-Pd-Pd (111) surface.

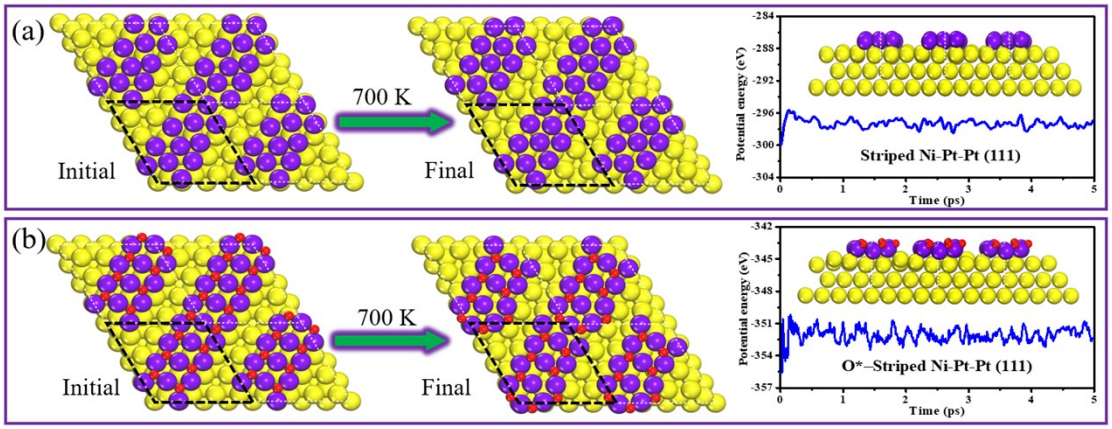

Figure S14. AIMD simulations for striped bimetallic surfaces Ni-Pt-Pt (111) at 700 K (a) without and (b) with adsorptive O atoms located at f1 and h2 sites. The rightmost insets in (a–b) show the potential energy fluctuation as a function of the simulated time. The side views of the final states are shown as insets for illustrations. The purple, yellow, and red spheres denote Ni, Pt, and O atoms, respectively. The black dashed quadrangle denotes the unit cell.

References

(1) J. Shen, G. Jones and T. Bligaard. Computational Research for Lean-Burn Direct NO Decomposition Catalysts – Final Report of Project Part 1, 2008.